Spin gapless armchair graphene nanoribbons under magnetic field and uniaxial strain*

Hou Hai-Ping(侯海平)[a)b)], Xie Yue-E(谢月娥)[a)b)†], Chen Yuan-Ping(陈元平)[a)b)], Ouyang Tao(欧阳滔)[a)b)], Ge Qing-Xia(葛青霞)[a)b)], and Zhong Jian-Xin(钟建新)[a)b)‡]

[a)] *Hunan Key Laboratory for Micro-Nano Energy Materials and Devices, Xiangtan University, Xiangtan* 411105, *China*

[b)] *Laboratory for Quantum Engineering and Micro-Nano Energy Technology and Faculty of Materials and Optoelectronic Physics, Xiangtan University, Xiangtan* 411105, *China*

(Received 5 November 2012; revised manuscript received 29 January 2013)

Using Green's function method, we investigate the spin transport properties of armchair graphene nanoribbons (AGNRs) under magnetic field and uniaxial strain. Our results show that it is very difficult to transform narrow AGNRs directly from semiconductor to spin gapless semiconductors (SGS) by applying magnetic fields. However, as a uniaxial strain is exerted on the nanoribbons, the AGNRs can transform to SGS by a small magnetic field. The combination mode between magnetic field and uniaxial strain displays a nonmonotonic arch-pattern relationship. In addition, we find that the combination mode is associated with the widths of nanoribbons, which exhibits group behaviors.

Keywords: graphene, spin gapless, spin transport, tight-binding

PACS: 73.63.–b, 85.75.–d, 85.35.–p **DOI:** 10.1088/1674-1056/22/8/087303

1. Introduction

Spin gapless semiconductors (SGS), in which spin valence band touches spin conduction band at the Fermi level, was proposed in 2008 based on gapless semiconductors.[1] They can create the fully spin-polarized (FSP) currents near the Fermi energy,[1,2] which is the most desirable and invaluable property for spintronics.[1–4] Therefore, the studies of SGS have aroused great interest.[1–5]

Graphene nanoribbons (GNRs) possess many excellent spin transport properties, such as high mobility,[6,7] weak spin–orbit coupling,[8–10] and long spin coherence time.[11] In two typical types of GNRs, i.e., armchair GNRs (AGNRs) and zigzag GNRs (ZGNRs), armchair GNRs (AGNRs) are energetically and thermodynamically more stable than ZGNRs.[12,13] Therefore exploring spin transport properties of AGNRs is more important. Previous studies have predicted that SGS can be realized in AGNRs by CH2 radicals attached at the edges of the nanoribbons.[5] However, such an extremely sensitive edge-dependent method requires the atomic-scale control of positions of CH2 radicals, which is very difficult to realize in experiment.[14,15] On the other hand, the energy region of spin polarization cannot be adjusted continuously by using this kind of method. Recently, some studies indicate that a magnetic field combined with uniaxial strain is an effective method to modulate the spin transport properties,[16–20] which can produce fully spin-polarized currents in the AGNRs.[16–18] For example, Soodchomshom and Chantngarm[17] proposed a normal/strained/ferromagnectic/normal graphene junction. The magnetic field induces a spin-polarized current while the polarization degree can be continuously modulated by strain. Using normal/strained/normal/ferromagnectic/normal graphene junction, Zhai *et al.*[19] found that a combination of the strain and magnetic modulations generates a valley-polarized current. The degree of the valley polarization can be tuned by the strain and a scalar potential. Niu[18] investigated the spin transport in ferromagnetic/strained/ferromagnetic graphene junction. He found that the junction can be used as a strain-tunable spin filter, because only the spin-down electrons are allowed to transmit, for the pseudo-vector potential caused by strains is in a range of 15 meV–25 meV.

Motivated by these studies, in this paper we study the spin transport in the strained AGNRs ($0 \sim 7.5$ nm wide) under uniform magnetic field. It is found that narrow AGNRs can be turned into SGS only under a magnetic field, but the magnetic field is too large to be realized in experiment. As a uniaxial strain is incorporated, AGNRs can present SGS behavior under a small magnetic field. This is due to the fact that the uniaxial strain reduces the band gaps of AGNRs. The relationship between magnetic field and uniaxial strain for achieving SGS is also investigated. We find that the magnetic field as a function of uniaxial strain displays a nonmonotonic-arch pattern. Moreover, the spin polarization region in SGS can be

*Project supported by the National Basic Research Program of China (Grant No. 2012CB921303), the National Natural Science Foundation of China (Grant Nos. 51172191, 11074211, 11074213, 51006086, and 51176161), and the Joint Funds of the Natural Science Foundation of Hunan Province, China (Grant No. 10JJ9001).

†Corresponding author. E-mail: xieyech@xtu.edu.cn

‡Corresponding author. E-mail: jxzhong@xtu.edu.cn

© 2013 Chinese Physical Society and IOP Publishing Ltd

tuned continuously by the combined effects of magnetic field and uniaxial strain. Finally, we discuss the dependence of SGS states in AGNR on the width of nanoribbon.

2. Model and method

Consider an AGNR under a magnetic field and uniaxial strain as shown in Fig. 1. The system can be divided into three regions: left lead, central region, and right lead. The width of the AGNR is labeled by W. The uniaxial strain is uniform along the armchair direction, and the magnetic field $B = (0,0,B_z)$ is perpendicular to the AGNR. We employ the π-orbital tight binding model to describe the spin transport properties of AGNRs.[21–23] The tight binding Hamiltonian of AGNRs can be expressed as[22,23]

$$H(B) = \sum_{is} \varepsilon_i c_{is}^{\dagger} c_{is} + \sum_{\langle ij\rangle,s} t_n \mathrm{e}^{\mathrm{i}2\pi\phi_{i,j}} c_{is}^{\dagger} c_{js} + g_s \sum_{is} c_{is}^{\dagger} (\sigma \cdot B) c_{is}, \quad (1)$$

where $c_{is}^{\dagger}$ and c_{is} are the creation and annihilation operators for an electron with spin s ($s = \uparrow, \downarrow$) on site i, respectively, and $\varepsilon_i = 0$ is the on-site energy.[23] The last term on the right-hand side of Eq. (1) is due to Zeeman energy. Here $g_s = (1/2) g \mu_{\mathrm{B}}$ (with $g = 4$) is the Lande g factor, phase $\phi_{i,j} = \int \boldsymbol{A} \cdot \mathrm{d}\boldsymbol{l}/\phi_0$ with vector $\boldsymbol{A} = (-B_z y, 0, 0)$, $\phi_0 = h/e$ being the quantum of flux, and $\sigma = \pm 1$ describes the up/down spin states. Due to the edge effects, there are four kinds of hopping energies labeled by t_n ($n = 1,2,3,4$) in Fig. 1, where $t_1 = -2.70$ eV and $t_2 = -2.65$ eV are the inner hopping energies and $t_3 = -3.20$ eV and $t_4 = -2.75$ eV are the edge hopping energies.[24,25] When a uniaxial strain is exerted along the armchair direction, the bonds deformation affects the hopping energies.[28–30] We use the change Δt of hopping energy t_1 to represent the strength of the strain ($\Delta t < 0$ eV and $\Delta t > 0$ eV correspond to compressive and tensile strains, respectively), then the changes in other hopping integrals are set to be $\Delta t_2 = 0.15\Delta t$, $\Delta t_3 = 0.40\Delta t$, and $\Delta t_4 = 0.13\Delta t$.[25]

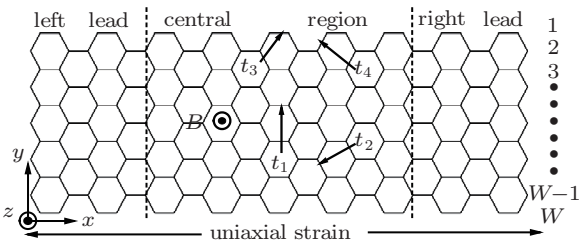


Fig. 1. Schematic of an AGNR with width $W = 11$, where the uniaxial strain is homogeneous along the armchair direction and the magnetic field $B = (0,0,B_z)$ is perpendicular to the AGNR.

The lattice Green's function method is used to calculate spin transport properties of the AGNRs. According to the Green's function scheme, the Green's function of the AGNRs can be expressed as[26,27]

$$\varsigma_r^{ss'}(E,B) = \left[EI - H_{\mathrm{C}}(B) - \Sigma_{\mathrm{L}}^{s}(E,B) - \Sigma_{\mathrm{R}}^{s'}(E,B)\right]^{-1}, \quad (2)$$

where $H_{\mathrm{C}}(B)$ is the Hamiltonian of the central region, $\Sigma_{\mathrm{L(R)}}^{s(s')}(E,B)$ is the self-energy of the left (right) lead that can be calculated by the recursive Green's function method. Once the total Green's function $\varsigma_r^{s(s')}(E,B)$ is obtained, the spin conductance from the left lead with spin s to the right lead with spin s' can be calculated by the following equations:[26,27]

$$G_{s's}(E,B) = \frac{e^2}{h} \mathrm{Tr}\left[\Gamma_{\mathrm{L}}^{s}(E,B)\, \varsigma_r^{ss'}(E,B)\, \Gamma_{\mathrm{R}}^{s'}(E,B) \left[\varsigma_r^{ss'}(E,B)\right]^{\dagger}\right], \quad (3)$$

where $\Gamma_{\mathrm{L(R)}}^{s(s')}(E,B) = \mathrm{i}\left\{\Sigma_{\mathrm{L(R)}}^{s(s')}(E,B) - \left[\Sigma_{\mathrm{L(R)}}^{s(s')}(E,B)\right]^{\dagger}\right\}$ is the coupling function of the left (right) lead. But the spin-flip effects induced by other factors are not considered in this work.

3. Results and discussion

In Fig. 2 we present the spin-dependent conductances for an AGNR ($W = 32$) under magnetic field. The conductances of spin-up and spin-down electrons are degenerate completely without magnetic field ($B = 0$) [see the inset in Fig. 2(a)]. When a magnetic field $B = 30$ T is exerted on the nanoribbon, a 100% spin polarization is produced at the spin-up and spin-down channels far away from the Fermi level as shown in Fig. 2(a). Meanwhile the spin-dependent band gap of the nanoribbon decreases from initial value ΔE_1 to ΔE_2. As the magnetic field increases to 100 T [see Fig. 2(b)], the spin-up channel shifts from left to right while the spin-down channel shows the opposite behavior. The polarization regions of spin-up and spin-down channels are extended with the increase of magnetic field, and the spin-dependent band gap further decreases to ΔE_3. When the magnetic field reaches 256.25 T, the spin-up channel touches the spin-down channel at the Fermi level, i.e., the band gap vanishes and the AGNR transforms from a semiconductor to an SGS.

According to the ribbons widths, AGNRs can be divided into three groups, i.e., $W = 3p$, $3p+1$, or $3p+2$, where p is an integer. Here, we chose $W = 30$, 31, and 32 ($p = 10$) to represent the three typical groups. Figure 3(a) shows the spin-dependent band gap ΔE of AGNRs as a function of magnetic field. It is found that the values of spin-dependent band gap ΔE decrease monotonically with the increase of magnetic field. The decreasing speeds of ΔE depend on the ribbon type ($31 > 32 > 30$). When the magnetic fields increase to certain values, all the AGNRs achieve zero spin-dependent band gaps.

It means that the AGNRs turn into SGS. The required magnetic fields for the AGNRs with width $W = 30$, 31, and 32 are 356.75, 391, and 256.25 T, respectively. But these magnetic fields are too large to be realized in the experiment. Considering that AGNRs have different initial spin-dependent band gaps, in Fig. 3(b) we show the variations of the ribbon width W with magnetic field strength and the AGNRs are all in SGS states. It can be found that the width decreases smoothly with the increase of magnetic field. Compared with the groups $3p$ and $3p+1$ with the same p value, the group $3p+2$ needs the smallest magnetic field to reach the SGS state. It is due to the fact that AGNR with width $W = 3p+2$ has the smallest initial spin-dependent band gap ΔE. As the nanoribbon becomes very wide, the magnetic field is insensitive to the variation of width. All nanoribbons need a magnetic field about $B = 100$ T to turn into the SGS. However, the magnetic field is still very large, which indicates that experimentally AGNRs cannot be transformed into the SGS only under the modification of magnetic field.

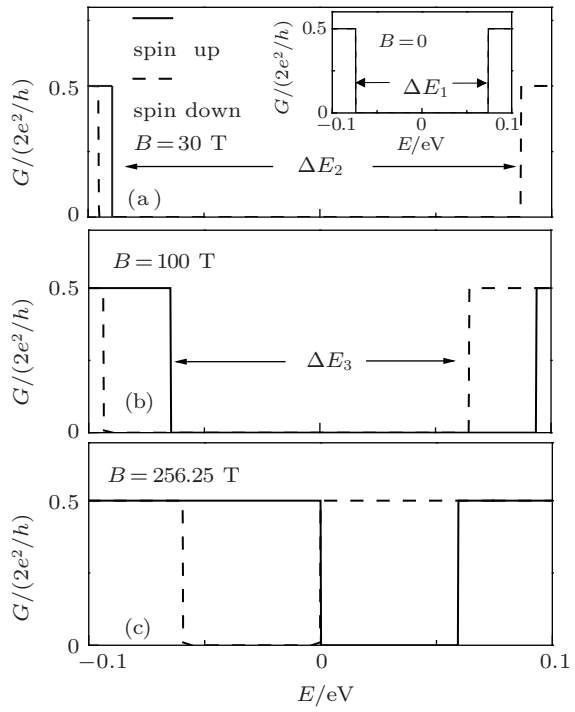


Fig. 2. Plots of spin-dependent conductance G versus electron energy E for a typical AGNR with $W = 32$, at $B = 30$ T (a), $B = 100$ T (b), and $B = 256.25$ T (c). The spin-up conductance is shown by the full line. The dashed line represents the spin-down conductance.

Due to the difficulty in experiment, we add uniaxial strain to help magnetic field drive semiconducting AGNRs into SGS states. The spin-dependent conductances of AGNR with width $W = 32$ are presented in Fig. 4. The uniaxial strain is set to be 0.06 eV and magnetic field is 30 T in Fig. 4(a). Comparing it with Fig. 2(a), one can find that both the spin-up channel and the spin-down channel move towards the Fermi level. The spin-dependent band gap of the nanoribbon decreases from ΔE_2 to $\Delta E_2'$. As uniaxial strain Δt increases to 0.087 eV, AGNR turns into SGS, in which the spin polarization channels split completely at the Fermi level. The size of the spin polarization region does not change with the increase of uniaxial strain Δt. When uniaxial strain is fixed ($\Delta t = 0.06$ eV), the comparison between Figs. 4(a) and 4(c) reveals that the spin polarization region extends with the increase of magnetic field and the spin-dependent band gap decreases from $\Delta E_2'$ to $\Delta E_3'$. The above phenomena are due to the fact that the uniaxial strain just modifies spin-dependent band gap[28–30] and the magnetic field can modulate both the spin-dependent band gap and the spin splitting position. These factors cause the spin channels of Fig. 4(d) to become wider than those of Fig. 4(b), when the AGNRs are at their SGS states.

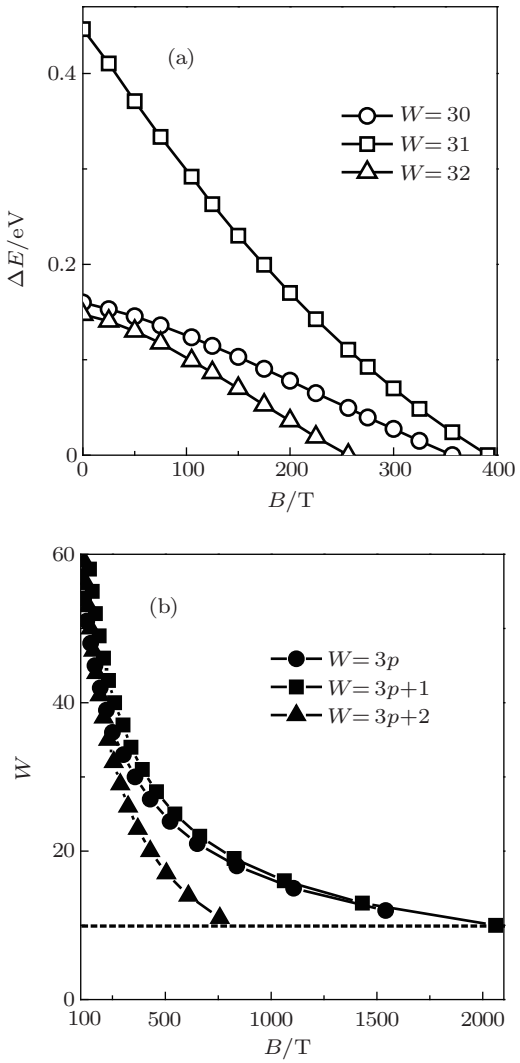


Fig. 3. (a) Band gaps for three typical AGNRs with widths $W = 30$, 31, and 32 varying with magnetic field. (b) Variations of AGNR width with magnetic field when the three typical AGNRs are in SGS states.

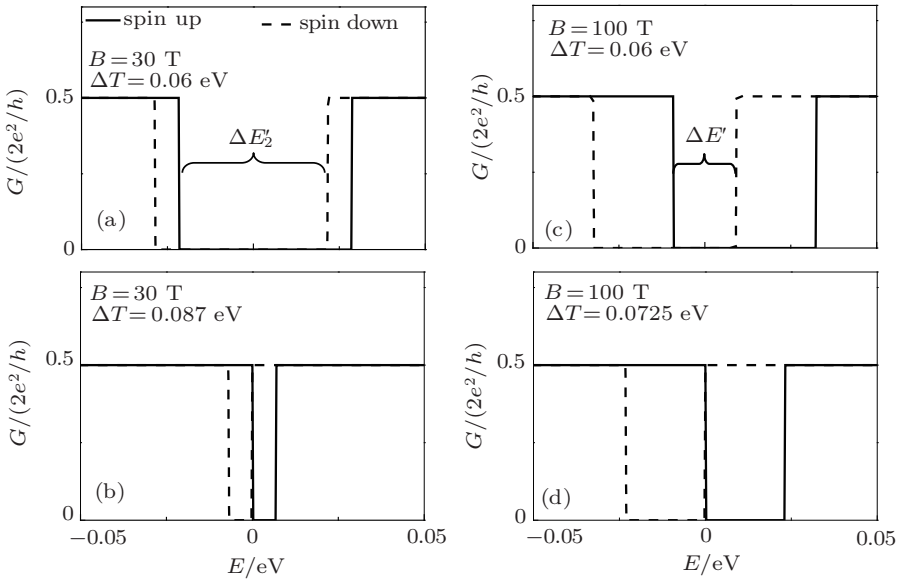


Fig. 4. Plots of spin-dependent conductance versus electron energy for a typical AGNR with $W = 32$.

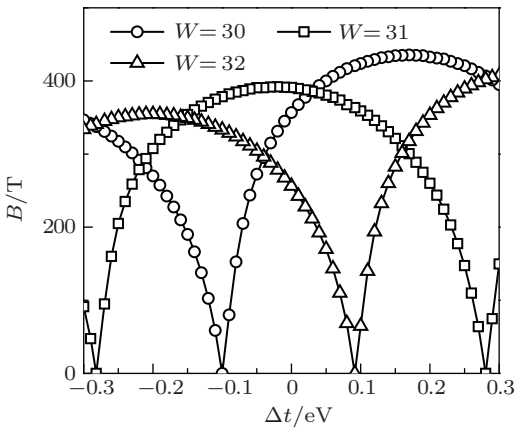


Fig. 5. Variations of magnetic field versus strain when the three typical AGNRs are in their SGS states.

To better understand the effect of strain on the spin transport, we further investigate the combination mode with strain and magnetic field, when AGNRs are in SGS states. Figure 5 illustrates the variations of magnetic intensity with strain for different widths. One can find that magnetic intensity is continuously variable. It indicates the regions of the spin-up or spin-down channels induced by Zeeman effects can be adjusted by the magnetic field continuously. This feature results from the fact that uniaxial strain can shift the position of the spin channels, which has been discussed in Fig. 4. All the curves of magnetic intensity for three different ribbon widths (W = 30, 31, and 32) each display an arch oscillation as the strain varies. It creates that several strains can match with a fixed magnetic field. But the three curves also exhibit distinct features with the variation of strain. As the strength of tensile strain is enhanced, the magnetic intensities for AGNRs with $W = 31$ and 32 first decrease to about zero and then increase. While the AGNR with $W = 30$ needs compressive strain first to display these behaviors. Particularly, the curve of AGNR with width $W = 31$ is almost symmetrical about the line crossing zero point. For magnetic field close to zero ($B = 1$ T), two strains ($\Delta t = -0.28015$ eV, 0.28016 eV) can match it. The strains for AGNRs with width $W = 30$ and 32 are -0.10015 eV and 0.0914 eV, respectively. Without magnetic field, three AGNRs would possess identical spin-dependent band gaps of about 0.05 meV introduced by these strains.

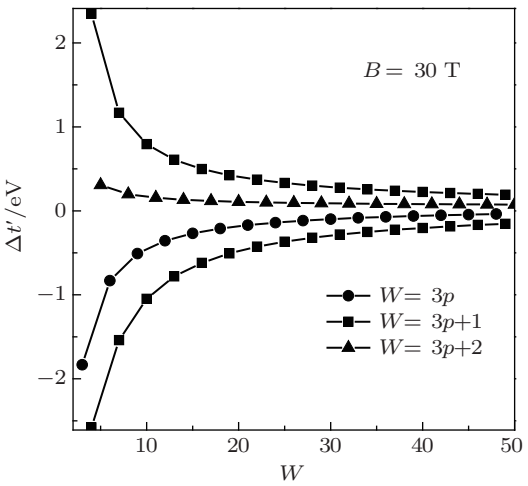


Fig. 6. Variations of the smallest strain in the combination mode of AGNRs with widths at $B = 30$ T.

Finally, we consider the effect of ribbon width on the smallest strain $\Delta t'$ in the combination mode. We calculate the variations of $\Delta t'$ in a magnetic field range of 0 T–100 T. Figure 6 shows the curves at a fixed magnetic field $B = 30$ T. It is clear that the smallest strains for AGNRs with width $W = 3p$ are compressive and those for AGNRs with width $W = 3p+2$

are tensile strains. However, the smallest strains for AGNRs with width $W = 3p+1$ can be compressive or tensile strains. Our results also show that the values of the smallest strain $\Delta t'$ for the three different AGNRs decrease smoothly with the increase of width. It is due to the fact that at a fixed magnetic field the gap size of AGNR scales with the inverse of ribbon width. Moreover, when the ribbon width is less than 60, the smallest uniaxial strain in the combination mode exhibits group behaviors, which depends on the ribbon width ($3p+1 > 3p > 3p+2$, $p = 1, 2, 3, \ldots$). A conclusion can be obtained that the AGNRs with widths $W = 3p+2$ are the most promising ribbons for reaching SGS states, since the uniaxial strains for them are smallest. To find quantitative values of $\Delta t'$ for the three AGNRs, we present a function as follows:

$$\Delta t' = A\exp(-W/B) + C\exp(-W/D) + E, \tag{4}$$

of which the parameters are presented in Table 1.

Table 1. Values of parameters ($\Delta t'$ is in unit eV, p is a positive integer and other parameters are dimensionless).

Ribbon kinds	$\Delta t'$ kinds	A	B	C	D	E
$W = 3p$	compressive	–0.857	11.747	–4.454	2.202	–0.0288
$W = 3p+1$	compressive	–4.75	3.304	–1.382	14.977	–0.106
	tensile	8.521	2.128	–1.208	12.052	0.1789
$W = 3p+2$	tensile	0.854	2.626	0.156	13.866	0.071

4. Conclusions

In this paper, we use the Green's function method to study the spin transport properties of AGNRs under perpendicular magnetic fields and uniform uniaxial strain distributions along the armchair direction. Our results indicate that when only perpendicular magnetic field is applied, AGNRs need unrealistic huge magnetic fields to achieve a kind of SGS. However, as a uniaxial strain is exerted on the nanoribbons, small magnetic fields can drive AGNRs into these ideal states. Under the combined effect of magnetic field and uniaxial strain, the size of the spin channel of SGS is continuously adjustable. The spin polarization direction can be manipulated by only tuning the gate voltage. Furthermore, we investigate the combination mode between magnetic field and uniaxial strain. The magnetic field modification as a function of uniaxial strain displays a nonmonotonic relationship with an arch pattern. Finally, we consider the effects of AGNRs widths on the combination mode. The results show that at a fixed magnetic field, the smallest uniaxial strain in the combination mode exhibits group behaviors. AGNRs with the widths $W = 3p+2$ ($p = 1, 2, 3, \ldots$) exhibit the most promising behavior for reaching SGS states, since the uniaxial strain for them is smallest.

References

[1] Wang X L 2008 *Phys. Rev. Lett.* **100** 156404
[2] Wang X L, Peleckis G, Zhang C, Kimura H and Dou S X 2009 *Adv. Mater.* **21** 2196
[3] Li Y F, Zhou Z, Shen P W and Chen Z F 2009 *ACS Nano* **3** 1952
[4] Pan Y and Yang Z 2010 *Phys. Rev. B* **82** 195308
[5] Pan Y and Yang Z 2011 *Chem. Phys. Lett.* **518** 104
[6] Li X, Wang X, Zhang L, Lee S and Dai H 2008 *Science* **319** 1229
[7] Wang X, Ouyang Y, Li X, Wang H, Guo J and Dai H 2008 *Phys. Rev. Lett.* **100** 206803
[8] Min H, Hill E J, Sinitsyn N A, Sahu B R, Kleinman L and MacDonald A H 2006 *Phys. Rev. B* **74** 165310
[9] Yao Y, Ye F, Qi L, Zhang S C and Fang Z 2007 *Phys. Rev. B* **75** 041401(R)
[10] Huertas-Hernando D, Guinea F and Brataas A 2006 *Phys. Rev. B* **74** 155426
[11] Tombros N, Jozsa C, Popinciuc M, Jonkman H T and Wees B J V 2007 *Nature* **448** 571
[12] Okada S 2008 *Phys. Rev. B* **77** 041408(R)
[13] Wassmann T, Seitsonen A P, Saitta A M, Lazzeri M and Mauri F 2008 *Phys. Rev. Lett.* **101** 096402
[14] Myoung N and Ihm G 2011 *J. Appl. Phys.* **109** 053716
[15] Lee Y L, Kim S, Park C, Ihm J and Son Y W 2010 *ACS Nano* **4** 1345
[16] Fujita T, Jalil M B A and Tan S G 2010 *Appl. Phys. Lett.* **97** 043508
[17] Soodchomshom B and Chantngarm P 2011 *J. Supercond. Nov. Magn.* **24** 1885
[18] Niu Z P 2012 *J. Appl. Phys.* **111** 103712
[19] Zhai F, Zhao X F, Chang K and Xu H Q 2010 *Phys. Rev. B* **82** 115442
[20] Soodchomshom B 2011 *Physica B* **406** 614
[21] Chen F, ChenY P, Zhang M and Zhong J X 2010 *Chin. Phys. B* **19** 086105
[22] Yu X X, Xie Y E, Ou Y T and Chen Y P 2012 *Chin. Phys. B* **21** 107202
[23] Zhen H Q, Jian W, Wei Y D and Guo H 2008 *Phys. Rev. Lett.* **101** 016804
[24] Son Y W, Cohen M L and Louie S G 2006 *Phys. Rev. Lett.* **97** 48216803
[25] Sun L, Li Q X, Ren H, Su H B, Shi Q W and Yang J L 2008 *J. Chem. Phys.* **129** 074704
[26] Chen Y P, Xie Y E, Sun L Z and Zhong J X 2008 *Appl. Phys. Lett.* **93** 092104
[27] Chen Y P, Xie Y E and Yan X H 2008 *J. Appl. Phys.* **103** 063711
[28] Gui G, Li J and Zhong J X 2008 *Phys. Rev. B* **78** 075435
[29] Li J, Gui G and Zhong J X 2008 *J. Appl. Phys.* **104** 094311
[30] Li J, Sun L Z and Zhong J X 2010 *Chin. Phys. Lett.* **27** 077101